Distribution of Induction, Electric Field, and Current Density, in Thin $YBa_2Cu_3O_{7-x}$ Films Carrying Transport Current

E. Sheriff, D. Giller, Y. Radzyner, A. Shaulov, Y. Schlesinger, and Y. Yeshurun

Institute of Superconductivity, Department of Physics, Bar-Ilan University, Ramat-Gan, 52900 Israel

An array of miniature Hall sensors has been utilized to measure the spatial distribution and time evolution of the local induction in a thin $YBa_2Cu_3O_{7-x}$ film at the remanent state, before and after the application of a dc transport current. As a result of transport current the induction peak is shifted from the center of the sample, indicating an inhomogeneous current distribution. Transport current markedly changes the spatial distribution of the electric field and the relaxation rate, creating a "dynamic neutral line" where the electric field is maximum, and the relaxation rate is zero.

PACS numbers: 74.76.Bz, 74.60.Ge

1. INTRODUCTION

The study of superconductors subjected to both transport current and external magnetic field is of fundamental as well as technological interest. Depending on the ratio I/I_c between transport and the critical current, three different states of the vortex system can be theoretically defined:[1] A pinned lattice ($I/I_c \ll 1$), a plastic flow regime ($I/I_c \leq 1$), and a 'moving vortex lattice' ($I/I_c \gg 1$). The transition from the plastic flow regime to the moving vortex lattice has attracted special interest.[2] Much less attention has been paid to the other limit ($I/I_c \ll 1$). Zeldov *et al.*[3] and Brandt *et al.*[4] treated this case theoretically, providing analytical expressions for the spatial distributions of the induction and of the current density. The time evolution of the induction profiles was treated by McElfresh *et al.*[5] Local magnetic measurements in the presence of transport current in the limit $I \ll I_c$ were preformed by McElfresh *et al.*[5] and Darwin *et al.*[6] using a single Hall probe. In this work we utilize an *array* of Hall probes (HPA) to measure the spatial distribution and time evolution of the magnetic induction across a thin $YBa_2Cu_3O_{7-x}$ (YBCO) film. An HPA was previously utilized by Fuchs *et al.*[7] employing an *ac* measuring technique. The focus in the present work is on the effects of *dc* transport currents in the limit $I \ll I_c$. From the measured spatial distribution and time evolution of the induction profiles we extract the spatial distributions of transport current and electric field across the sample, and determine the effects of transport current on the *local* magnetic relaxation.

2. EXPERIMENTAL

Current leads were attached onto an epitaxial YBCO film (dimensions: $600 \times 2200 \times 0.3$ μm^3, $T_c \simeq 90$ K), laser ablated on a $SrTiO_3$ substrate, with the *c*-axis perpendicular to the film plane. The sample was mounted on an HPA, containing nine elements each with a 30×30 μm^2 active area. Probe #1 was located just outside the sample and probe #7 near the sample center.

After zero-field-cooling the sample to a preset temperature below T_c, an external magnetic field was ramped up to a level higher than twice the full penetration field, and then removed. The relaxation of the local magnetic induction in the remanent state was monitored for approximately 430 seconds by each of the nine Hall-probes. Subsequently, a dc transport current was switched on and the relaxation was measured for additional 600 seconds.

3. RESULTS

Fig. 1 shows typical induction profiles at 87 K, before and after the application of 100 mA transport current. The effects of transport current are clearly observed: The peak is suppressed, and shifted from the center of the sample, causing an asymmetric field profile. These features are enhanced as transport current and/or temperature are increased. The induction field resulting from a homogeneous current distribution superimposed on a symmetric induction profile cannot affect the location of the peak. Thus, the shift of the induction peak from the center is a clear indication of an inhomogeneous current distribution.

The spatial distribution of the relaxation rate is also affected by the transport current. Prior to application of the transport current, the relaxation rate exhibits a maximum at the sample's center and changes sign at

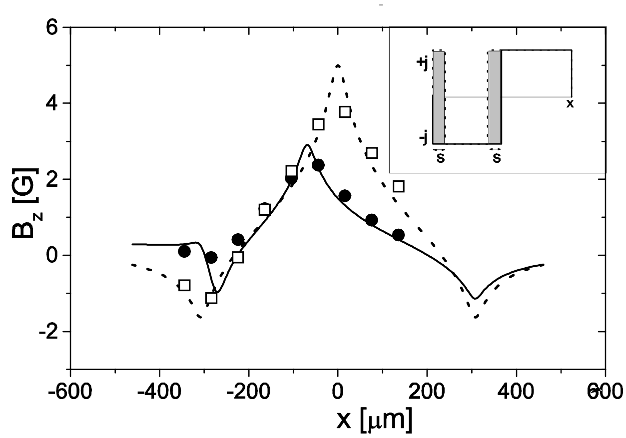

Fig. 1. Induction profiles at 87 K before (open squares) and after (solid circles) application of 100 mA transport current. Center is located at $x = 0$. Lines are theoretical fits using approximated current distributions as shown in the inset: Transport current causes addition of two current sheets (grey rectangles) to pre-existing current distribution.

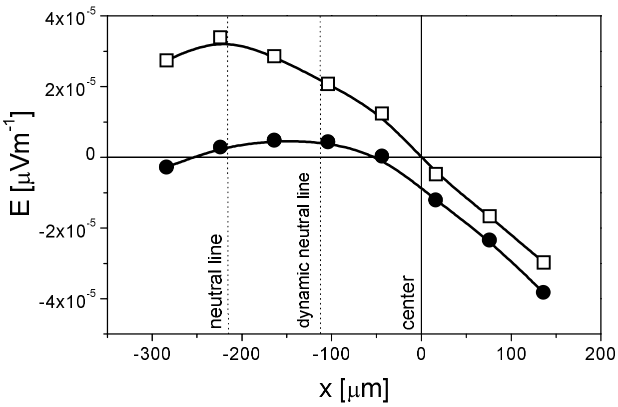

Fig. 2. Profiles of electrical field 15 seconds after removal of magnetic field (open squares) and 15 seconds after application of 100 mA transport current (solid circles) at 86 K. Lines are guide to the eye.

the 'neutral line'[8,9]where B_z changes sign. As a result of the transport current, a new 'dynamic neutral line' is created, across which the relaxation rate changes sign although B_z does not change sign. The dynamic neutral line is located closer to the center than the neutral line, and its position depends on the magnitude of the transport current. It is difficult in our experiment to locate the dynamic neutral line on the basis of the raw relaxation data because noise introduces large error bars in $\partial B_z/\partial t$ in the regime where $\partial B_z/\partial t \simeq 0$. Spatial integration of the relaxation data, which yields the electric field,[10] reduces the noise, clearly revealing the dynamic neutral line. Fig. 2 shows the spatial distribution of the electric field E, as calculated from the relaxation data, $E = -1/c \int (\partial B_z/\partial t)\, dx$. The integration constant is calculated by taking $E = 0$ where the current changes its sign, namely at the location of maximum B_z. Note that before application of transport current, E is zero at the sample center and maximum at the neutral line,[8,9] where B_z changes sign and $\partial B_z/\partial t = 0$. After application of the transport current, E is crossing the zero line at two points around the dynamic neutral line, where E is maximum and the relaxation rate diminishes. Note also that at the dynamic neutral line the relaxation rate changes sign although B_z does not change sign.

4. ANALYSIS AND DISCUSSION

Following Zeldov *et al.*[3,4] and McElfresh *et al.*[5] we assume that a positive transport current affects only the side of the sample where the shielding current is negative. This is based on the assumption that in the time window of our experiment the critical current can be replaced by the persistent current. We approximate their calculated current distribution by adding two current sheets of width s to the original (no transport current) distribution (see inset to fig. 1). The persistent current is extracted by fitting the measured induction profiles to those arising from the assumed current distribution. The fits shown in fig. 1 yield quite reasonable agreement with the data, taking s to be 40 μm. The value of s increases with time, temperature and transport current, as expected.

The measured profiles of the electric field (fig. 2) are consistent with the above description of the current distribution. The zero points of E correspond to the points where the current density changes sign. In-between these two points, E reaches a maximum where the relaxation rate diminishes in accordance with the rate equation $\partial B_z/\partial t = -c\partial E/\partial x$. The existence of such a "dynamic neutral line" can be understood by considering the time evolution of s: as j decays, s increases. Simple analysis shows that the increase in s compensates for the decay in B_z at the dynamic neutral line.

The location of the dynamic neutral line is approximately given by the intersection of the remanent state induction profile and the induction profile due to transport current alone in the absence of pinning.

ACKNOWLEDGMENTS

This work was supported by the Israel Science Foundations and by the Heinrich Hertz Minerva Center for High Temperature Superconductivity. Y.Y. and A.S. acknowledge support from the USA-Israel Bi-National Science Foundation.

REFERENCES

1. A. E. Koshelev and V. M. Vinokur, Phys. Rev. Lett. **73**, 3580 (1994); L. Balents and M. P. A. Fisher, Phys. Rev. Lett. **75**, 4270 (1995); T. Giamarchi and P. Le Doussal, Phys. Rev. Lett. **76**, 3408 (1996); S. Ryu *et al.*, Phys. Rev. Lett. **77**, 5114 (1996); L. Balents *et al.*, Phys. Rev. Lett. **78**, 751 (1997); S. Scheidl and V. M. Vinokur, Phys. Rev. B **56**, 8522 (1997).
2. M. C. Hellerqvist *et al.*, Phys. Rev. Lett. **76**, 4022 (1996); U. Yaron *et al.*, Nature **376**, 753 (1995).
3. E. Zeldov *et al.*, Phys. Rev. B **49**, 9802 (1994).
4. E. H. Brandt and M. V. Indenbom, Phys. Rev. B **48**, 12893 (1993); E. H. Brandt *et al.*, Europhys. Lett. **22**, 735, and E. H. Brandt, Phys. Rev. B **49**, 9023 (1994).
5. M. McElfresh *et al.*, Phys. Rev. B **51**, 9111-9117 (1995).
6. M. Darwin *et al.*, Phys. Rev. B **48**, 13192 (1993).
7. D. T. Fuchs *et al.*, Nature **391**, 373 (1998).
8. Y. Abulafia *et al.*, in *Coherence in High Temperature Superconductors*, A. Revcolevschi and G. Deutcher eds. World Science Publishing, p. 297, (1995); Y. Abulafia *et al.*, Phys. Rev. Lett. **75**, 2404 (1995).
9. T. Schuster, H. Kuhn, and E. H. Brandt, Phys. Rev. B **51,** 697 (1995).
10. Y. Abulafia *et al.*, Physica C **282-287**, 2225 (1997); D. Giller *et al.* Phys. Rev. B **57**, 14080 (1998).